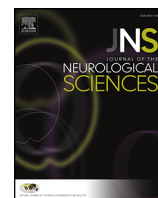




Contents lists available at ScienceDirect

Journal of the Neurological Sciences

journal homepage: www.elsevier.com/locate/jns

Inhibition of inflammation with celastrol fails to improve muscle function in dysferlin-deficient A/J mice

Blythe C. Dillingham^{a,1}, Margaret E. Benny Klimek^a, Ramkishore Gernapudi^{a,1}, Sree Rayavarapu^a, Eduard Gallardo^b, Jack H. Van der Meulen^b, Sarah Jordan^b, Beryl Ampong^b, Heather Gordish-Dressman^b, Christopher F. Spurney^b, Kanneboyina Nagaraju^{a,c,*}

^a Research Center for Genetic Medicine, Children's National Medical Center, 111 Michigan Ave NW, Washington, D.C., USA

^b Institut de Recerca Hospital de la Santa Creu i Sant Pau. U.A.B.C./Pare Claret, 167 08025 Barcelona, Spain

^c Department of Integrative Systems Biology, Institute for Biomedical Sciences, The George Washington University, 2300 Eye Street, N.W., Ross 605, Washington, D.C., USA

ARTICLE INFO

Article history:

Received 27 November 2013

Received in revised form 18 June 2015

Accepted 22 June 2015

Available online xxx

Keywords:

Muscular dystrophy

Skeletal muscle

Dysferlin

Celastrol

NF- κ B

Inflammation

ABSTRACT

The dysferlin-deficient A/J mouse strain represents a homologous model for limb-girdle muscular dystrophy 2B. We evaluated the disease phenotype in 10 month old A/J mice compared to two dysferlin-sufficient, C57BL/6 and A/JolaHsd, mouse lines to determine which functional end-points are sufficiently sensitive to define the disease phenotype for use in preclinical studies in the A/J strain. A/J mice had significantly lower open field behavioral activity (horizontal activity, total distance, movement time and vertical activity) when compared to C57BL/6 and A/JolaHsd mice. Both A/J and A/JolaHsd mice showed decreases in latency to fall with rotarod compared to C57BL/6. No changes were detected in grip strength, force measurements or motor coordination between these three groups. Furthermore, we have found that A/J muscle shows significantly increased levels of the pro-inflammatory cytokine TNF- α when compared to C57BL/6 mice, indicating an activation of NF- κ B signaling as part of the inflammatory response in dysferlin-deficient muscle. Therefore, we assessed the effect of celastrol (a potent NF- κ B inhibitor) on the disease phenotype in female A/J mice. Celastrol treatment for four months significantly reduced the inflammation in A/J muscle; however, it had no beneficial effect in improving muscle function, as assessed by grip strength, open field activity, and *in vitro* force contraction. In fact, celastrol treated mice showed a decrease in body mass, hindlimb grip strength and maximal EDL force. These findings suggest that inhibition of inflammation alone may not be sufficient to improve the muscle disease phenotype in dysferlin-deficient mice and may require combination therapies that target membrane stability to achieve a functional improvement in skeletal muscle.

© 2015 Elsevier B.V. All rights reserved.

1. Introduction

Dysferlinopathies are autosomal recessive muscle disorders caused by mutations in the dysferlin (*DYSF*) gene [1–3]. Predominant phenotypes associated with mutations in the *DYSF* gene include limb girdle muscular dystrophy 2B (LGMD2B) and Miyoshi myopathy (MM). Both LGMD2B and MM are slow progressing, late-onset dysferlinopathies; LGMD2B patients present with proximal muscle weakness, while MM patients initially show weakness in distal muscles. Histologically, muscle biopsies show myofiber degeneration as well as significant inflammation, including accumulation of macrophages, CD8⁺ T cells, and CD4⁺ T cells [4]. Currently, several genetic approaches are being tested

in the hope of attaining curative treatment for dysferlinopathies, including exon skipping and trans-splicing; however, these techniques are in their infancy and will take time to move to human clinical trials [5–8]. Even if these therapies are successful, it is likely that they will not be completely curative because of differential correction in various muscles. Genetic alteration to dysferlin could have effects on specific protein interaction sites in the Dysferlin protein. Therefore, the use of palliative therapeutic approaches using pharmacological and immunological agents to modulate dysferlin-associated pathology would be a more effective and useful approach either alone or in combination with other therapies.

Animal models of human disease play an important role in understanding disease pathogenesis, identification of drug targets and evaluation of therapeutic efficacy of drugs in preclinical trials. Therefore, characterization of disease phenotypes in these animal models would help us better interpret the results of preclinical trials. Several dysferlin mouse strains exist; these include: Bla/J, A/J, C57BL/6J-Chr6^{A/J}/NaJ, SJL/J, and B10.SJL-Dysfm/AwaJ. Of these, the A/J and SJL/J strains have

* Corresponding author at: Professor of Integrative Systems Biology and Pediatrics Children's National Medical Center, 111 Michigan Avenue, N.W., Washington, DC 20010, USA.

E-mail address: knagaraju@childrensnational.org (K. Nagaraju).

¹ Equal contribution.

spontaneous mutations in the dysferlin gene [9–15]. More specifically, A/J mice have an ETn retrotransposon inserted into intron 4 of the dysferlin gene and develop histological evidence of muscular dystrophy after 4 to 5 months of age. These mice show slow progression of disease pathology with persistent muscle weakness [9]. By 14 months of age, the muscles of A/J mice show marked inflammatory and fatty infiltration and significant muscle degeneration. The A/J strain is one of the commercially available models used to understand pathogenesis of dysferlin deficiency [9].

The presence of inflammatory infiltrates in dysferlin-deficient muscle suggests their prominent role in muscle pathology. Recent reports indicate that pro-inflammatory nuclear factor κ B (NF- κ B) is upregulated in dysferlin-deficient myotubes [16]. Celestrol is a triterpene derived from the plant *Tripterygium wilfordii*, the “thunder god vine,” and has been used in traditional Chinese medicine for its anti-inflammatory effects. Celestrol has been shown to suppress I κ B phosphorylation and NF- κ B activation by inhibiting TAK1 activation [17]. We have previously developed a muscle-based NF- κ B inhibitor screening assay and shown that celestrol is one of the powerful inhibitors of NF- κ B under this system [18]. Based on this data, inhibition of NF- κ B anti-inflammatory agents such as celestrol to suppress immune activation in dysferlin-deficient muscle could ameliorate the disease pathology. In this study, the phenotypes of dysferlin-deficient A/J mice were compared to dysferlin-sufficient C57BL/6 and A/JOlaHsd mice using well-established functional and behavioral assessments. Using these assays, we also tested the effect of celestrol on muscle disease phenotype in dysferlin-deficient A/J mice.

2. Materials and methods

2.1. Animals

All mice were handled according to local institutional animal care and use committee guidelines. For the phenotyping experiments examining the differences in functional and behavioral measures between normal and diseased mice, A/JOlaHsd ($n = 7$) were purchased from Harlan laboratories (Indianapolis, IN). A/J ($n = 8$) and C57BL/6 ($n = 12$) mice were purchased from the Jackson Laboratories (Bar Harbor, ME). All mice examined in phenotyping experiments were 9 months old and groups contained the following numbers of males and females: A/JOlaHsd ($n = 7$, 3 females & 4 males), A/J ($n = 8$, 4 females & 4 males) and C57BL/6 ($n = 12$, 6 females & 6 males). For pre-clinical evaluation of celestrol, 10 month old female A/J mice ($n = 20$) were purchased from the Jackson Laboratories. All mice were housed in an individually vented cage system with a 12-h light–dark cycle and received free access to standard mouse chow and water.

2.2. Administration of celestrol

Female A/J mice were randomly separated into two groups, untreated ($n = 7$) and celestrol-treated ($n = 13$). The untreated group received untreated water, whereas the treatment group received water with celestrol. The drug was administered in the drinking water for 4 months at a concentration of 8.6 μ g/mL. Celestrol-supplemented water was replaced three times a week, and water consumption was closely monitored throughout the trial. Body weight as well as functional and behavioral measures were monitored at 14 months of age and are described in detail below. At the end of the trial, mice were euthanized, and various muscle tissues were collected for histological evaluations. *In vitro* muscle force was also monitored to assess the effect of the drug on muscle function.

2.3. Functional tests

Functional and behavioral tests were performed to monitor the disease phenotype and to assess the effect of celestrol treatment, as

described previously [15,19]. Grip strength was assessed for both the fore- and hindlimbs, and the data are expressed as kg force/kg body weight (KGF/kg). Motor coordination (Rotarod) was monitored as described previously [15]. The length of time that each mouse stayed on the rod was recorded as latency to fall (sec), and the mean values obtained for each group were compared. Open-field behavioral activity was measured using an open-field Digiscan apparatus (Omnitech Electronics, Columbus, Ohio), as described previously [15,19]. Data were collected every 10 min over a period of one hour each day over four consecutive days. Total distance (cm), movement time (seconds), rest time (seconds), vertical activity (units), and horizontal activity (units) were expressed as mean \pm SEM.

2.4. *In vitro* force measurement

EDL muscles of the right hindlimbs were removed from anesthetized mice, and muscle mass was recorded (mg). Maximal force and the specific force produced by the EDL muscle were monitored as described previously [15,19]. The maximal force generated by the EDL was measured and represented as milliNewtons (mN). The specific force was assessed by dividing the maximal force by the cross-sectional area of the muscle and expressed in kN/m² [20] and expressed as mean \pm SEM.

2.5. Measurement of pro-inflammatory transcripts in A/J mice

The expression levels of NF- κ B target genes were determined using qPCR. Quadriceps tissues were obtained from 10- to 12-month-old A/J and C57BL/6 mice ($n = 3$ /group). Total RNA was isolated using the TRIzol reagent (Life Technologies) according to the manufacturer's instructions. cDNA was synthesized using a Life Technologies High Capacity cDNA Reverse Transcription Kit with RNase Inhibitor (Life Technologies Cat#4374966). qPCR was performed using an Applied Biosystems 7900HT Real-Time PCR machine. TaqMan probe sets TNF- α (Mm00443260_g1), MCP1 (Mm00441242_m1), IL6, HPRT, and 18S (4319413E) were purchased from Applied Biosystems. Relative induction was calculated using the $\Delta\Delta$ Ct method, with 18S or HPRT as the internal reference gene. Fold changes were expressed as means \pm SEM and statistical analysis was performed on the raw delta Ct values using the non-parametric Wilcoxon rank sum test.

2.6. Histological evaluations

Quadriceps muscles collected in formalin were used for hematoxylin and eosin (H&E) staining. The muscles were sent to Histoserv, Inc. (Germantown, MD) for staining. Digital images were taken at 20 \times magnification on an Olympus BX61 bright-field microscope and processed using Image J (NIH), with additional threshold plug-ins to process jpeg images. Pixels corresponding to non-muscle areas were highlighted and normalized to the total pixel area of the tissue image. Based on these values, we derived the muscle area and expressed the results as percentages. To quantify inflammation, stained sections were viewed using bright-field microscopy, and inflammatory foci per section were counted at 40 \times magnification. Inflammatory foci were defined as a group of 10 blue infiltrating nuclei in the muscle tissue. Entire tissue sections were quantified in a blinded fashion. Results were expressed as means \pm SEM.

2.7. Echocardiography

Echocardiography was performed as described previously [21–23]. Qualitative and quantitative measurements were made offline using analytic software (VisualSonics, Toronto, Ontario, Canada). Electrocardiogram kHz-based visualization (EKV) software analysis produced offline reconstruction for simulated 250- to 1000-Hz static and cine-loop images. Echocardiography measurements included vessel diameters, ventricular chamber size, and blood flow velocities across the

Download English Version:

<https://daneshyari.com/en/article/8275612>

Download Persian Version:

<https://daneshyari.com/article/8275612>

[Daneshyari.com](https://daneshyari.com)